CONNECTIONS OF AUDITORY MEDIAL BELT CORTEX IN MARMOSET MONKEYS

By

Lisa de la Mothe

Thesis

Submitted to the Faculty of the

Graduate School of Vanderbilt University

in partial fulfillment of the requirements

for the degree of

MASTER OF ARTS

in

Psychology

August, 2006

Nashville, Tennessee

Approved:

Jon Howard Kaas

Troy Alan Hackett

TABLE OF CONTENTS

LIST OF TABLES

LIST OF FIGURES

LIST OF ABBREVIATIONS

A1	primary auditory field/ auditory area 1
AL	anterolateral belt area
AS	arcuate sulcus
BDA	biotinylated dextroamine
BF	best frequency
CF	characteristic frequency
CiS	circular sulcus
CL	caudolateral belt area
CM	caudomedial belt area
CPB	caudal parabelt
CS	central sulcus
CTB	cholera toxin-B
D	doral division of the medial geniculate complex
DY	diamidino yellow
FB	fast blue
FE	fluoroemerald
FR	fluororuby
FRA	frequency response area
ILS	inferior limiting sulcus
INS	insula
IPS	intraparietal sulcus
Lim	limitans
LS	lateral sulcus
LuS	lunate sulcus
M	magnocellualr division of the medial geniculate complex
MD	medial dorsal nucleus
MGC	medial geniculate complex
MGd	dorsal division of the medial geniculate
MGm	magnocellular division of the medial geniculate
MGv	ventral division of the medial geniculate
ML	middle lateral belt area
Po	posterior group
Pro	proisocortex
proA	prokoniocortical area
PS	principal sulcus
Pv	parvalbumin
R	rostral area
reIt	retroinsular temporal cortex
RL	rostolateral field
RM	rostromedial belt area
RPB	rostral parabelt
RT	rostrotemporal area
RTL	rostrotemporal lateral belt area
RTM	rostrotemporal medial belt area
S2	somatosensory area 2
Sg	supragenicuIate
STG	superior temporal gyrus
STS	superior temporal sulcus
V	ventral division of the medial geniculate complex
VP	ventroposterior nucleus

CHAPTER I

INTRODUCTION

Current models of auditory cortex organization in primates emphasize the Old World macaque monkey, but are also reinforced by comparative observations in several New World species, including marmoset, owl, and squirrel monkeys. Based on the collective findings of the field the current working model divides the auditory cortex into three levels of processing which include a primary core region, a secondary belt region and a third level of processing in the parabelt region (Figure 1). A fourth level of processing is also thought to exist, which encompasses connections to the superior temporal sulcus, rostral superior temporal gyrus, and prefrontal cortex (Kaas & Hackett, 2000).

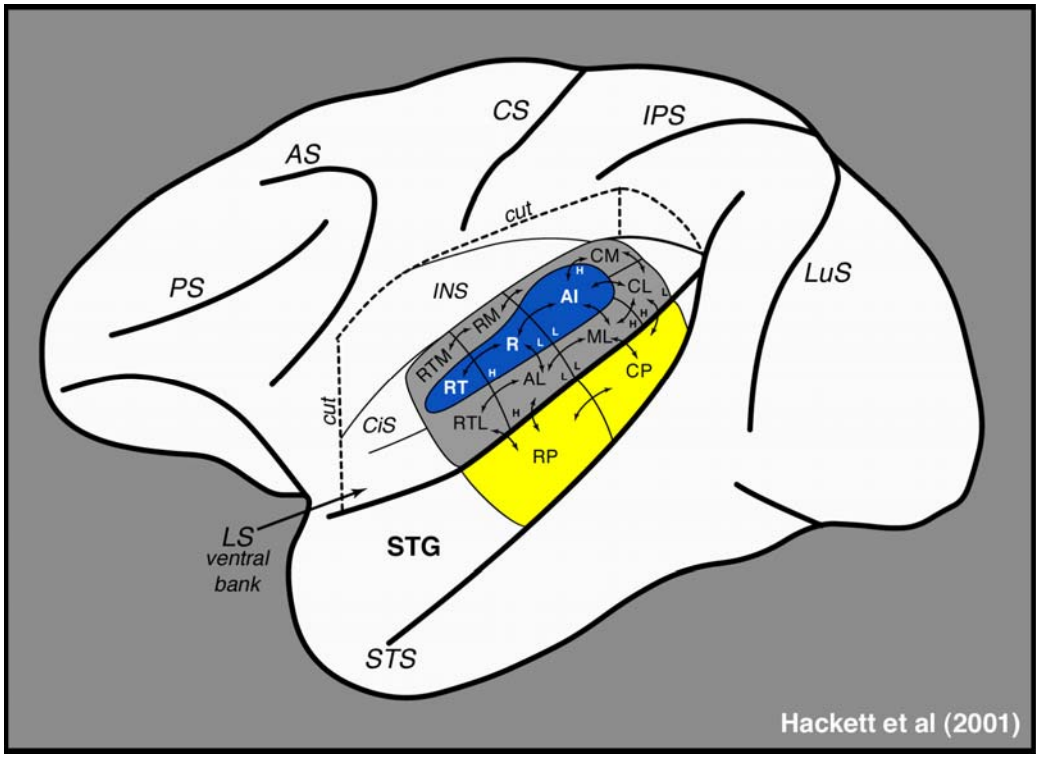

Figure 1. Diagram of current auditory processing model.

The core region is subdivided into three areas, A1, R and RT, which can be identified by architectonic characteristics typical of primary sensory areas including; koniocortical cytoarchitecture, dense astriate myelination, as well as dense expression of acetylcholinesterase, cytochrome oxidase, and parvalbumin (Morel &Kaas, 1992, Hackett et al., 1998). All areas of the core receive independent parallel inputs from the ventral medial geniculate (MGv) and thus process information in parallel (Rauschecker et. al 1997). The core areas are cochleotopically organized by characteristic frequency with isorepresentation curved. In A1 the low frequency representation is rostral and the high frequency representation caudal (Figure 1) (Kaas & Hackett, 1998; Kaas and Hackett, 2000). This gradient is reversed in R which shares a low frequency border with A1 and a high frequencies border with RT. The core areas project primarily to the belt areas where strongest connections are between adjacent areas and only weak projections to the parabelt (Hackett et al., 1998).

Surrounding the core both medially and laterally is the belt region which is divided into seven or more areas. Some of those areas are distinguished on the basis of physiological profiles and connection patterns (CL, ML, AL, CM), while others are based solely on connection patterns (RM, RTM, RTL). Medially to the core lie areas CM, RM, and RTM. Areas CL, ML, AL, and RTL border the core laterally. The belt has been shown to have strong interconnections with the core as well as other belt areas (Merzenich & Brugge 1973, Atkin et al. 1988, Morel & Kaas 1992). Thalamic connections to the belt areas come from the dorsal (MGd) and the magnocellular (MGm) divisions of the medial geniculate body, however, it appears to depend on the core for activation from cortical inputs (Kaas & Hackett, 2000). Projections from the belt area distribute principally to the parabelt (Kaas & Hackett,1998). The lateral belt areas are the most well studied and respond better to narrow bands than pure tones (Rauschecker et al. 1995). This preference for more complex stimuli is thought to apply to the medial belt areas (Rauschecker et al., 1997), but the location deep within the lateral sulcus has made this region difficult to study**.**

The parabelt is located lateral to the lateral belt on the dorsal surface of the superior temporal gyrus and receives strong projections from the belt areas (Kaas & Hackett 1998). Those caudal

belt areas that border A1 project to the caudal parabelt, whereas the rostral areas bordering R and RT project to the rostral parabelt (Kaas & Hackett, 1998). Area RM in the belt appears to be the only area that does not follow this rostral caudal topography as it projects to both rostral and caudal divisions of the parabelt, (Kaas & Hackett 1998). Thalamic connections of the parabelt include the MGd and MGm as well as the suprageniculate/limitans (Sg) and the medial pulvinar nuclei (Hackett et al. 1998b). There are no projections from the MGv or the core area (Hackett et al. 1998) and thus the parabelt receives auditory input either through thalamic projections from non-primary nuclei or more from the belt areas. The cortical connection patterns place the parabelt at a third level of processing (Kaas & Hackett 1998).

In our working model of auditory cortex organization, the anatomical and physiological properties of the belt areas medial to the core are the least well understood due in part to the narrow width of these areas, and their location deep within the lateral sulcus which presents numerous experimental challenges. Accordingly, the connections of the medial belt fields are only partially known from tracer injections made in other cortical fields. The principle aim of the present study was refinement of the working model with respect to the contribution of medial belt areas, which appear to be functionally distinct from lateral belt areas (Jones & Burton, 1976; Schroeder et al., 2001), but has not yet been systematically studied in any primate. Recent physiological evidence suggests that there may be auditory and somatic sensory convergence in at least one medial belt area, CM, (Schroeder et al., 2001), but a source of somatic sensory input to CM has not been identified. Although the medial belt is situated between primary auditory and secondary somatic sensory cortex (e.g., S2), projections from somatic sensory cortex are not known to target the medial belt. In the absence of somatic sensory cortical inputs, one hypothesis is that multisensory or somatic nuclei in the thalamus may drive responses to somatic stimulation in the medial belt. A subcortical multisensory auditory pathway projects in a diffuse manner to the entire auditory cortex, via inputs from the MGm, yet there is some evidence that projections from the MGm (multisensory pathway) may favor the medial belt fields (Jones and Burton, 1976). This study focuses on the connections of the medial belt areas RM and CM, in order to reveal the possible functional differences between medial and lateral belt areas, and also to investigate

possible differences between rostral and caudal medial belt areas. Experiments were conducted for this study in the marmoset for two initial reasons. First, access to the medial belt is less problematic than in macaques. Second, in recent years cortical coding of vocal communication sounds have been intensively studied in marmoset monkeys (Wang, 2000), yet little is known about auditory cortex organization beyond the core region in this primate.

CHAPTER II

METHOD

General Procedures

In eight marmoset monkeys (Callithrix jacchus jacchus) microinjections of up to five anatomical tracers were made into subdivisions of auditory cortex (Table 1) under aseptic conditions and in accordance to the Vanderbilt University Animal Care and Committee Guidelines and the Animal Welfare Act. Marmosets were premedicated with cefazolin (25mg/kg), dexamethozone (2mg/kg), cimetidine HCl (5mg/kg), and robinul (0.015mg/kg). Anesthesia was induced by inhalation of 5% isoflurane and the animals were intubated and maintained with less than 2% isoflurane and Nitrous Oxide with Oxygen (50/50) 1 liter/minute or ketamine/xylazine. Body temperature was maintained at 37°C with a water circulating heating pad. Vital signs were continuously monitored throughout the surgery and were used to adjust the levels of anesthesia.

Table 1. Summary of marmoset cases, injections made and tracers used.

	Medial Belt				**Core**		**Lateral Belt**				**Parabelt**	
Case	CM	RM	RTM	A1	R	RT	CL	ML	AL	RTL	RPB	CPB
01_37		**BDA**			**FE,FR**			**FB**	**FB**			
01_89	**CTB**						FR				DY	DY
01_118	**CTB**	**BDA**			**FR**		**FB**					
02_17	**CTB**	**CTB**										
02_51				**CTB**	FR							
02_60	CTB/N			FR								FB
02_75	CTB/N											FB
03_02	**BDA**								FR		FB	

A stereotaxic instrument (David Kopf Instruments, Tujunga, CA) was used to stabilize the head of the monkey. A midline incision was made exposing the skull, followed by the retraction of the left temporal muscle. A crainiotomy was performed exposing the superior temporal gyrus and the lateral sulcus, followed by the cutting and retraction of the dura. Warm saline was applied periodically to the brain to prevent dessication of the cortex during photography and injections of tracers. Photographs were then taken to facilitate later reconstruction of the injection sites based on blood vessels and sulci. Injections of up to five tracers were made using a 2μL syringe attached to a hydraulic microdrive injection sites were located using one of two procedures. First, monitoring of neuron response properties to locate auditory areas in penetrations through parietal cortex. Second, retraction of the parietal cortex, and using landmarks and blood vessels to locate auditory areas and make the injections directly into these areas (Figure 2). The tracers used were biotinylated dextroamine (BDA); cholera toxin-B (CTB); fast blue (FB); fluororuby (FR); diamidino yellow (DY); and fluoroemerald (FE). Due to the various levels of sensitivity of the tracers the amounts and solution concentrations were varied accordingly (typically, 0.01-0.05 μL and 3% fluorescents, 1% for CTB and 10% for BDA). The exposed area of the brain was covered with softened gelfilm, the crainiotomy was closed with dental acrylic, and the overlying temporal muscle and skin sutured back into place. Antibiotic gel was applied along the suture line. After the surgery, the endotracheal tube was removed and vital signs were monitored during the recovery period until vitals became stable and the animal was returned to its cage where it was monitored until recovery was complete. Daily injections of penicillin G (10 000 units i. m.) were giving for 5 to 7 days after surgery, along with Banamine (1 mg/kg) as needed for analgesia.

At the end of the survival period, a mapping session in which electrophysiological data was recorded in non-sterile surgical procedures occurred (Figure 3, Figure 4). Upon completion of the recording session a lethal dose of pentobarbital was administered. Just before cardiac arrest the animal was perfused through the heart with warm saline followed by cold 2% paraformaldehyde dissolved in 0.1 M phosphate buffer. Immediately following the perfusion the brains were removed and photographed, the two hemispheres and the brainstem were separated and placed in 30% sucrose for several days and then blocked. The hemispheres were cut

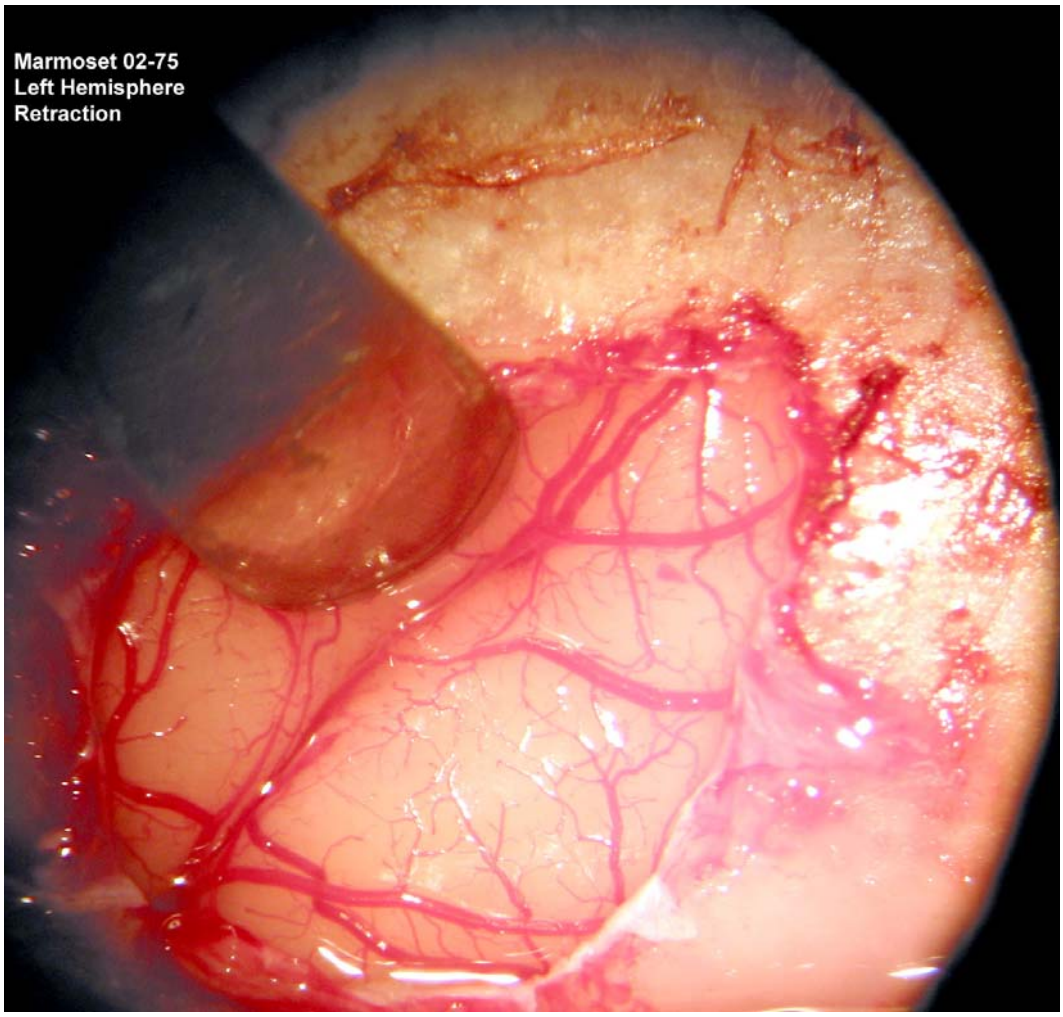

Figure 2. Photo of retraction of parietal cortex.

perpendicular to the lateral sulcus in either caudal to rostral, or rostral to caudal direction at 40 μm. Depending on the case, series of sections were processed for: (i) fluorescent microscopy; (ii) BDA (Sakai et al., 1996); (iii) CTB (iv) myelin (Gallyas, 1979); (v) acetylcholinesterase (Geneser-Jensen & Blackstad, 1971); (vi) stained for Nissl substance with thionin.

Data Analysis

Cells labeled with fluorescent, CTB and BDA tracers were all plotted on an X-Y plotter (Neurolucida) coupled to a Leitz microscope where fluorescents were potted under ultraviolet illumination. Photographs and drawings of each section were made, noting architectonic

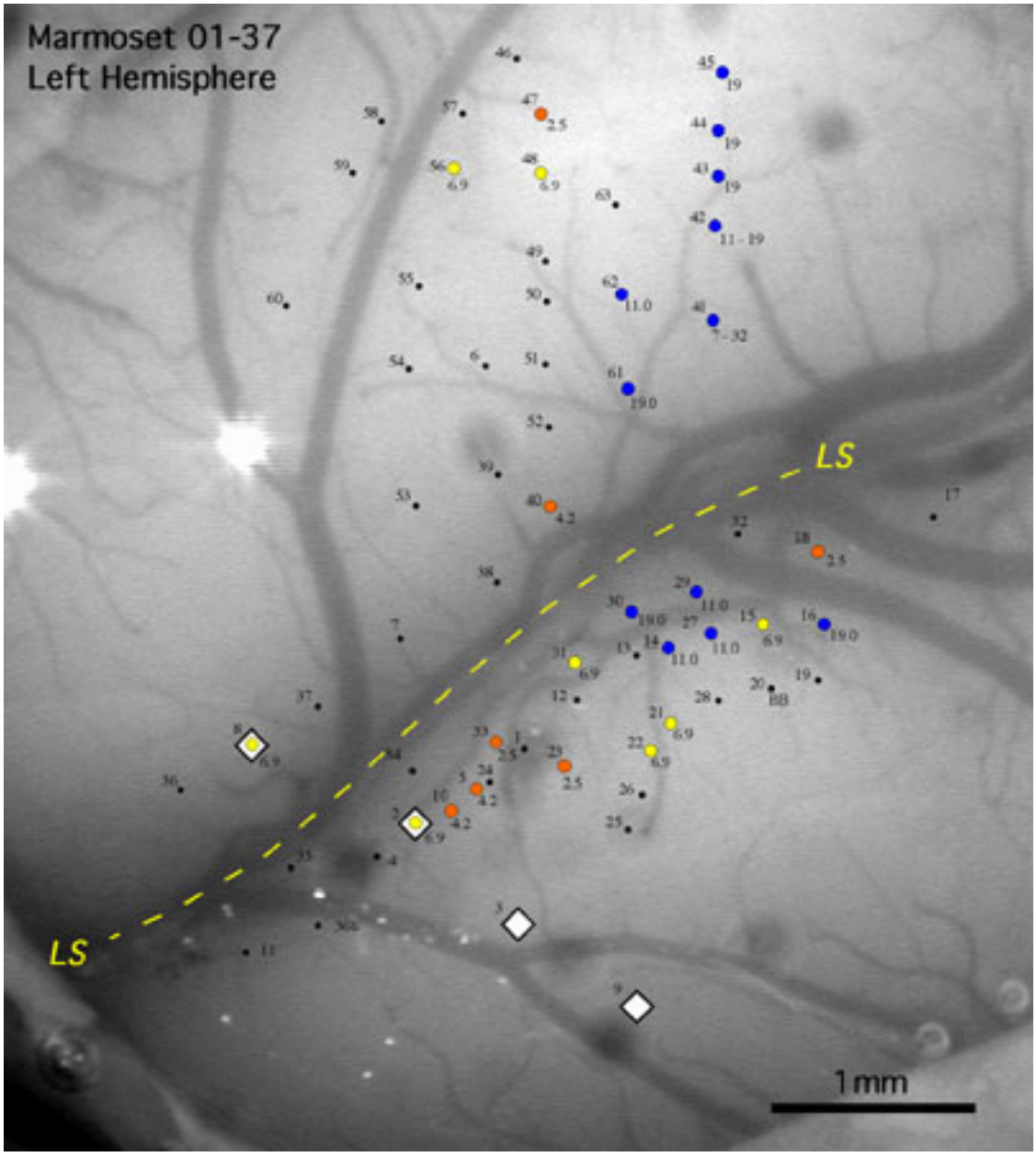

Figure 3. Image of the left hemisphere (ipsilateral) of marmoset auditory cortex and electrode penetrations with characteristic frequencies of neuron response properties. Blue circles > 10kHz, yellow circles > 5 < 10 kHz, orange circles < 5kHz. Injection sites are marked with diamonds and a dashed white line marks the lateral sulcus (LS).

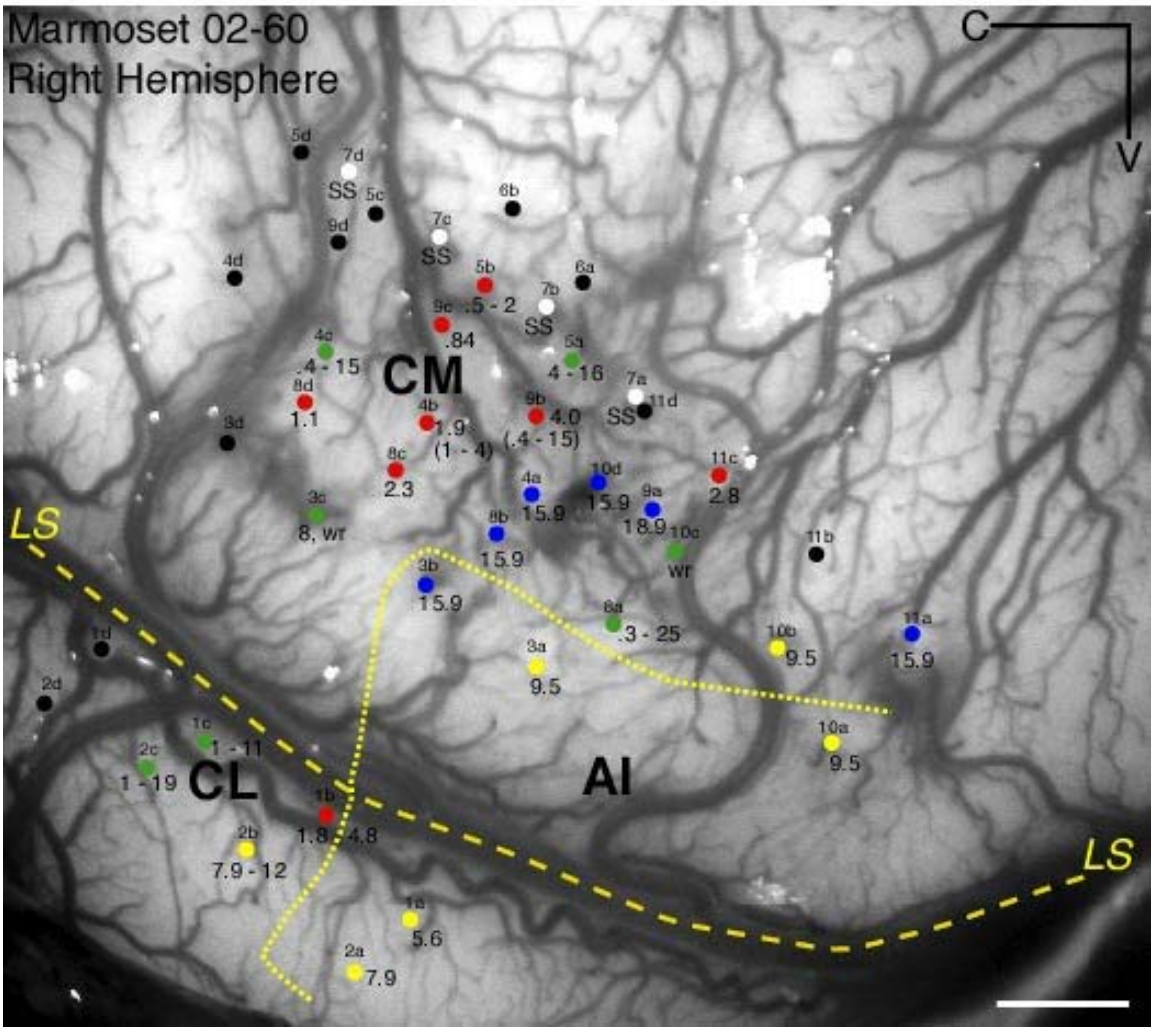

Figure 4. Image of the right hemisphere (contralateral) of marmoset auditory cortex and electrode penetrations with characteristic frequencies of neuron response properties. Numbers indicate penetration and characteristic frequency. Black dots represent penetrations with no response to pure tones.

boundaries, the location of blood vessels and the distribution of labeled cells. A composite drawing was made from adjacent sections processed for label, acetylcholinesterase, myelin, and Nissl by aligning common architectonic borders and blood vessels (Figure 5, Figure 6). Reconstructions of the composite images were achieved using Canvas 7.0 software (Deneba software, Miami, FL, USA). The final composites were analyzed to reveal the individual

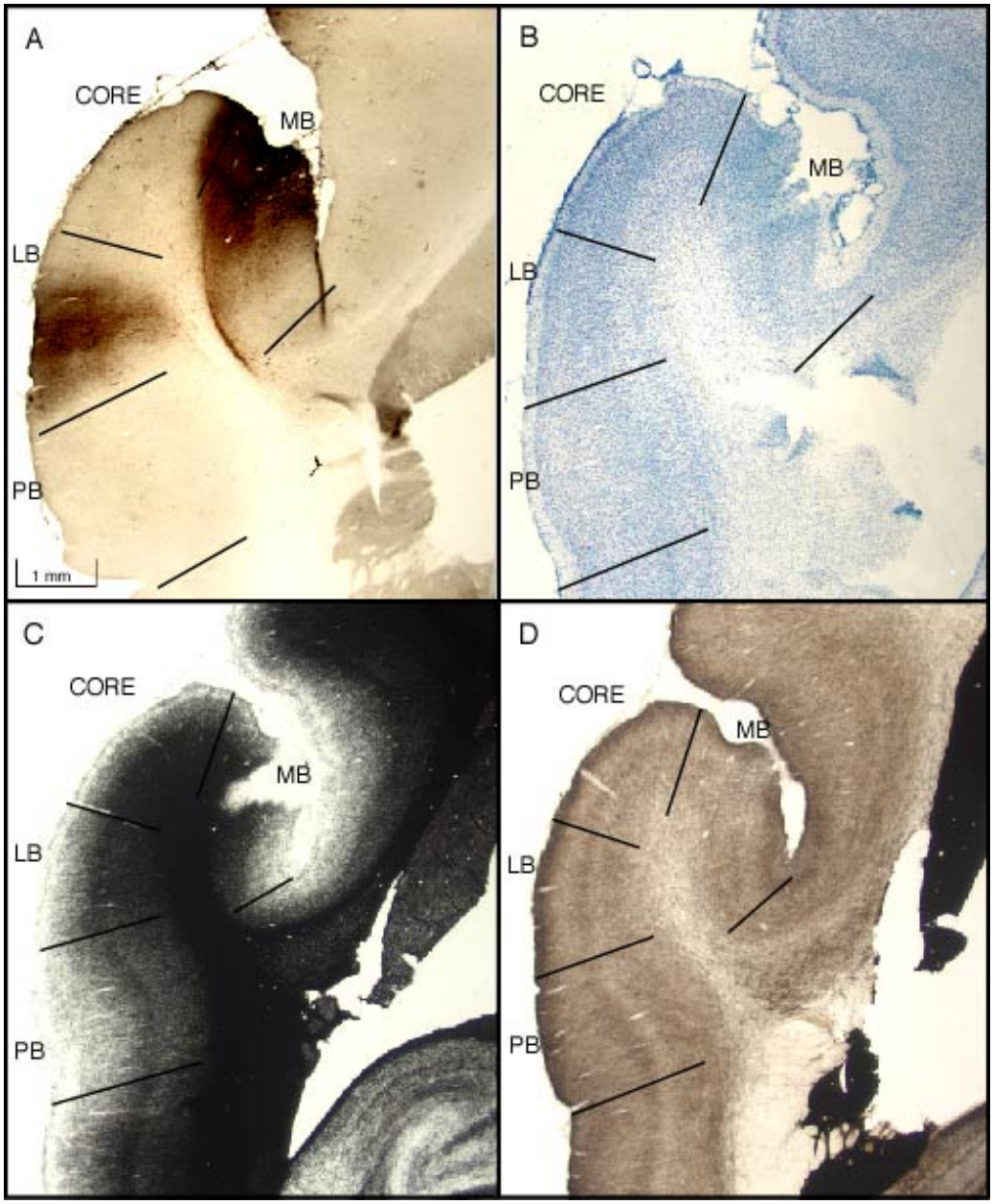

Figure 5. Architecture of marmoset auditory cortex showing borders (lines) between the borders of the medial belt, core, lateral belt, and parabelt regions. A: Biotinylated Dextroamine. B: Thionin stain for Nissl substance. C: Myelin stain. D: Acetylcholinesterase histochemistry. PB:parabelt, MB:medial belt, LB: lateral belt.

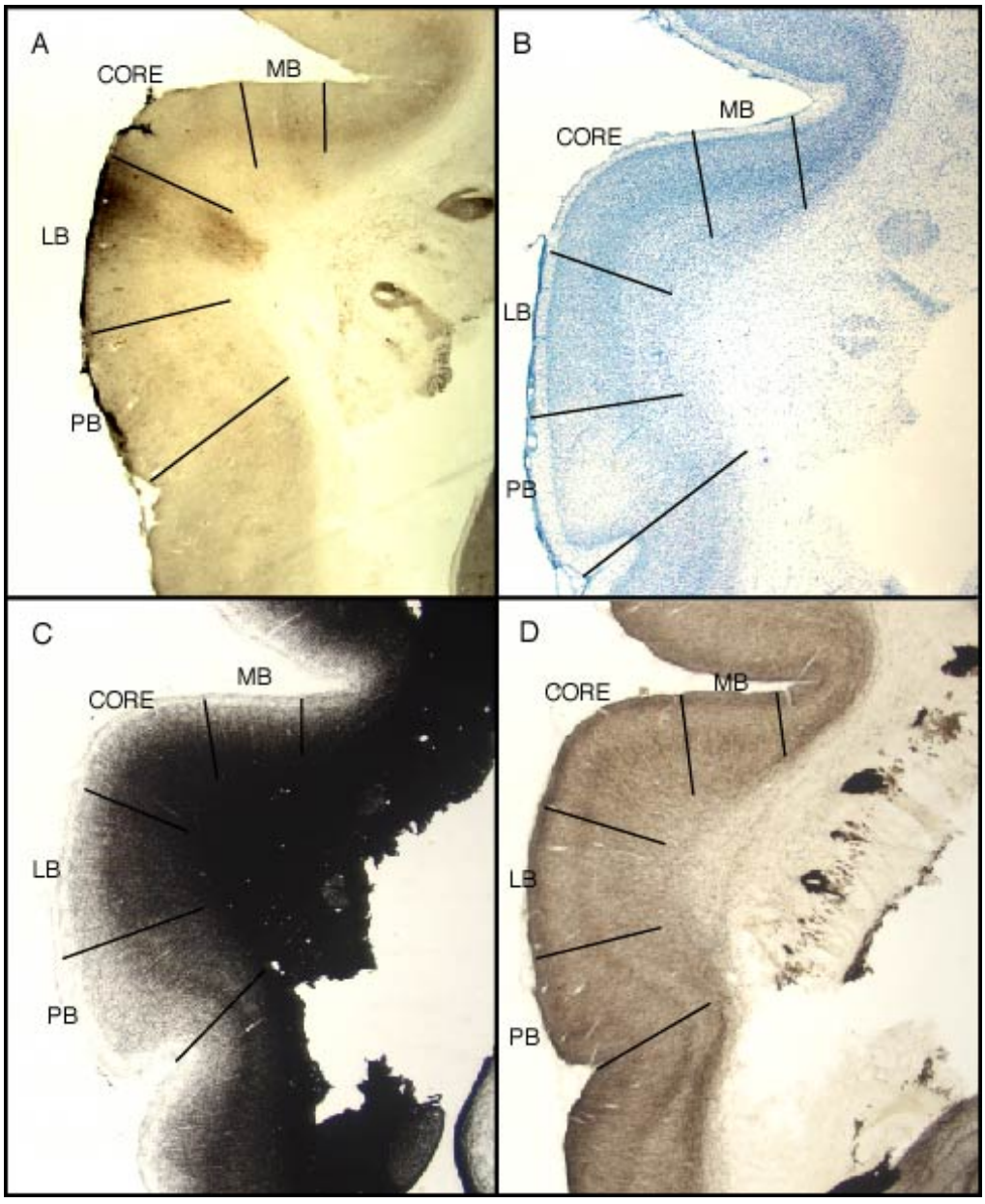

Figure 6. More caudal representations of the architectural borders (lines) of the subdivisions of the marmoset auditory cortex. The figure is approximately 2.2mm caudal from figure 1. A: Biotinylated Dextroamine. B: Thinonin stain for Nissl. C: Myelin stain. D: Acetylcholinesterase histochemistry. PB:parabelt, MB:medial belt, LB: lateral belt.

connection patterns and the connection patterns of injections at similar or dissimilar locations (Figure 7).

Figure 7. Composite figures of the auditory cortex (01-37) with borders defined through architectural identification as shown in figure 1a and 1b and all tracer injections present. Filled circles represent BDA medial belt injection (RM). Open circles represent Fluoroemerald (FE) core injection (R). Open triangles represent Fluororuby (FR) core injection (R). Open squares represent Fast Blue lateral belt injection (ML). Asterisks represent double labeling of FR and FE. Shaded gray areas represent anterograde from the BDA injection. Injections sites are shaded black and labeled accordingly. Numbers below composites represent the BDA section form which the image was compiled, lower numbers are more rostral, higher numbers more caudal. PB:parabelt, MB:medial belt, LB lateral belt.

Photographs were made using a Spot-2 camera mounted on a Nikon E8U05 microscope and adjusted for brightness, contrast, text added, and cropped using Adobe Photoshop v6.0 software (Mountain View, CA, USA). Other than the adjustments mentioned, the images were not altered in any way.

Auditory stimulation

Pure-tone and noise band acoustic stimuli were generated using a Tucker-Davis Technologies (Gainesville, FL) System II hardware and software. Auditory stimulation was accomplished by coupling STAX earphones to hollow ear bars affixed to the stereotaxic frame

(David Kopf Instruments, Tujunga CA). Stimuli were calibrated with a 1/4" microphone (ACO Pacific) controlled by SigCal software and hardware (Tucker-Davis). Amplitude corrections were saved in a data file and applied to each stimulus to flatten the response of each earphone independently. Stimulus presentation was controlled by the data acquisition software (see below). For each recording site the frequency response area (FRA) of the neuron or neuron cluster was obtained by presentation of a pure tone series (200 Hz to 40 kHz, 0.75 log steps) at each of several intensities (0 to 60 dB SPL, 10 or 15 dB steps). Each frequency-intensity combination was presented five times consecutively at a rate of 1 Hz. At sites that did not respond well to pure-tone stimuli (e.g., belt cortex), an additional FRA was usually obtained using 1/3-octave band stimuli. Center frequencies and intensities were the same as for pure tones.

Data acquisition and analysis

Single- and multi-unit recordings were made with1 MOhm tungsten microelectrodes oriented perpendicular to the pial surface. For sites on the gyral surface the electrode angle ranged from about 30 to 45 degrees. Penetrations targeting the lower bank of the lateral sulcus were made by a vertical approach through the overlying parietal cortex. The angle of penetration for these sites was slightly oblique, depending on location within the lateral sulcus. Neurons in layer III and IV were targeted by advancing the electrode in 50 um steps from the pial surface with a hydraulic microdrive (David Kopf Instruments, Tujunga CA). Stimulus presentation and data acquisition were controlled by Brainware software (Jan Schnupp, Tucker-Davis Technologies) and Tucker-Davis neurophysiology hardware. In most electrode penetrations, single channel recordings were made, but in some penetrations, multi channel recordings were made simultaneously from electrodes at approximately the same depth and separated by about 0.5mm. Spike data were stored on a computer hard drive for offline sorting and analysis (Matlab). Best frequency (BF, stimulus frequency generating the greatest number of spikes) and characteristic frequency (CF, stimulus frequency that elicited a reliable response at threshold) were determined for each recording site. Threshold could not be determined for some locations because neurons were responsive at levels below the noise floor of the system (-10 dB SPL). In

these cases, CF was estimated as the BF at 0 or –10 dB SPL. Response rasters and FRA plots were made from these analyses.

CHAPTER III

RESULTS

Architecture

Boundaries between subdivisions of the auditory cortex were determined by previously established architectonic criteria (Hackett et al. 1998, Hackett et al. 2001). The core area was identified by several features including dense myelination of layers III-VI constituting an astriate pattern, the inner and outer striae (layers IV & Vb) are not visible. In sections stained for Nissl substance the core area was characterized by a dense population of small to medium size cells and a wide granular layer IV and dominance of small pyramidal cells in layer three. Acetylcholinesterase, which has been demonstrated to be highly expressed in the core area of macaques, chimpanzees and humans (Hackett et al. 2001) was not found to have the same intensity of expression in marmosets and therefore was not as useful as a marker of the core. Thus, the intensity of acetylcholinesterase compared to other primate, in marmosets was more similar to that of the surrounding belt areas.

The architectural profile of the belt areas (lateral, medial and para) could be differentiated from the core by the bistriate pattern in which layers IV and Vb are visible. In myelin stained sections the borders of the lateral belt and parabelt could be distinguished mainly by the weak myelination of the upper (supragranular) layers in the parabelt. In the Nissl stain the size of layer III pyramidal cells increased dramatically at the border between core and belt areas. The larger cells were present in all belt areas including the parabelt. In the parabelt these cells were organized into orderly columns in and large pyramidal cells were more numerous in layer V.

In addition to architectonic features, boundaries between subdivisions of the auditory cortex were revealed by neuron response properties. The core subdivisions of A1 and R were distinguished by a reversal of the tonotopic gradient (Figure 3).

Neuron Response Properties

Core and belt neurons were distinguished by response thresholds and tuning band widths. Neurons in the core responded well to pure tones, with narrow tuning to frequency and low thresholds (Figure 8), whereas belt areas (Figure 9) typically exhibited broad tuning bands and higher thresholds.

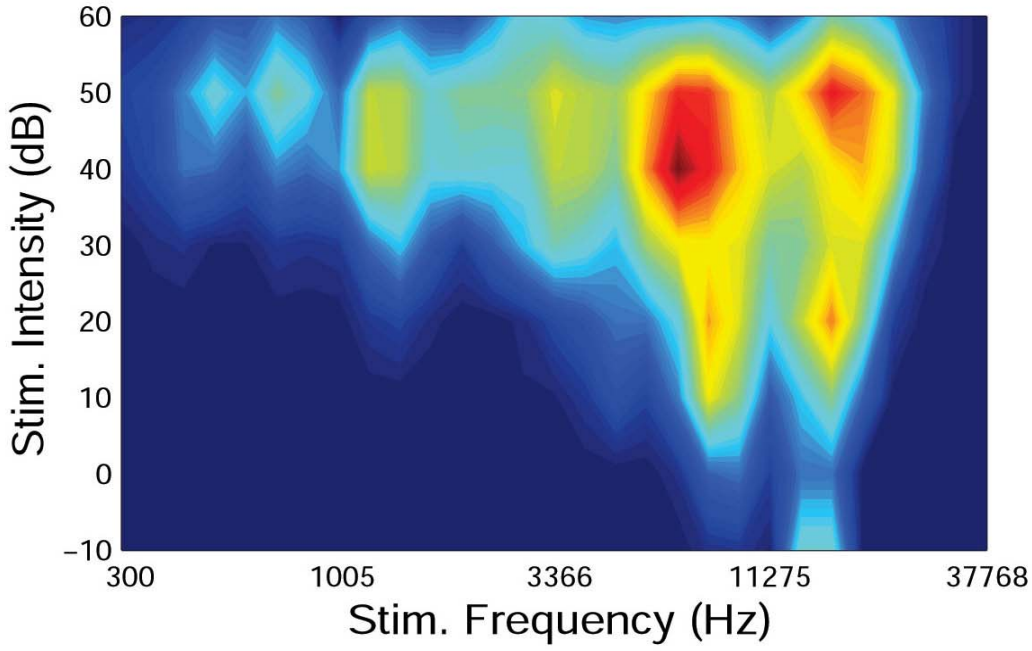

Figure 8. FRA core point.

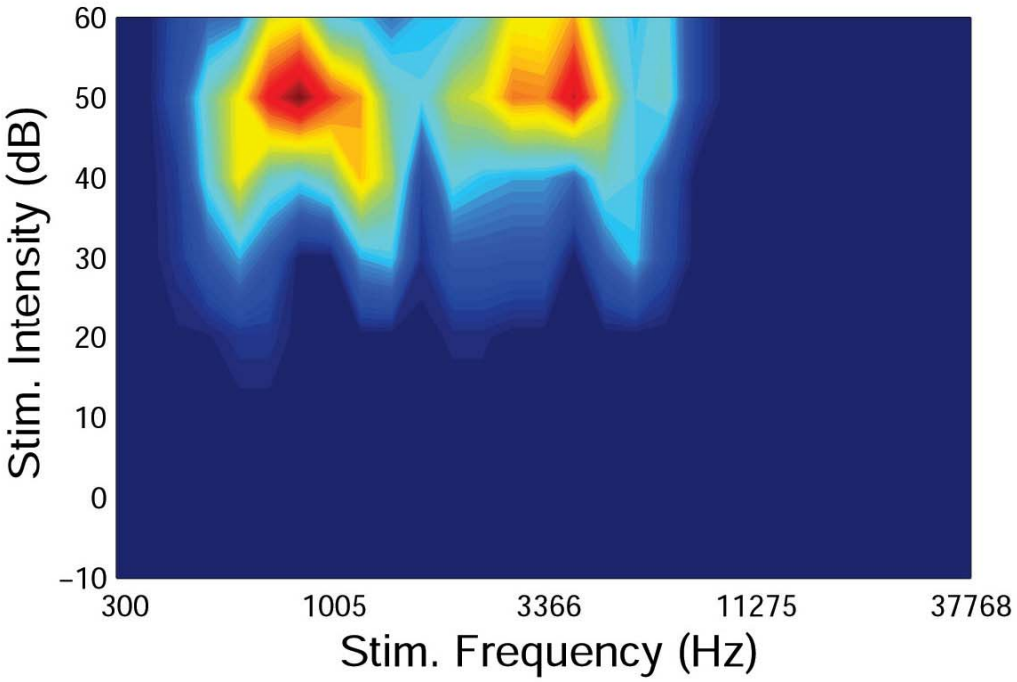

Figure 9. FRA belt point.

Connection Patterns

Injections of the rostral medial belt (RM) (cases 01-37, 01-118 BDA) labeled cells in the core, medial belt, lateral belt and parabelt (Figure 7). Anterograde and retrograde label was most heavily concentrated in the medial belt around the rostral medial belt injection site (Figure 10). Weaker labeling was found rostrally in the medial belt and there was an absence of label in the more caudal areas of the medial belt (Figure 10). Strong anterograde and retrograde labeling was found throughout the rostral and caudal divisions of the core. The extreme rostral areas of the lateral belt had anterograde labeling only, while there was strong bidirectional transport throughout the majority of the remaining lateral belt areas. Weak retrograde connections were found at the most caudal end of the lateral belt. There were strong retrograde and anterograde connections with patches of neurons in the rostral and caudal parabelt areas (Figure 10).

An especially interesting finding associated with the injection of the medial belt was the lack of connections in the lateral part of the core. Both anterograde and retrograde labeling

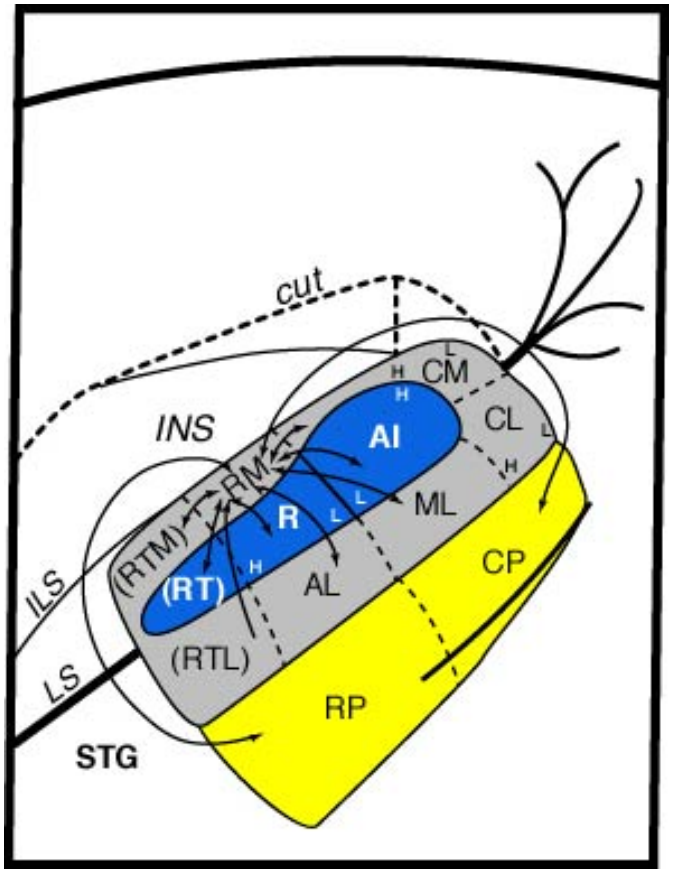

Figure 10. Summary figure of the medial belt (RM) injection connection pattern.

occurred in the medial portion of the core and left a gap in the lateral portion of the core while connections continued in the lateral belt (Figure 11). Differentiation of connections of medial and lateral halves of the core areas was not found after either the core injections or the lateral belt injections. In the architecture of the core we were unable to consistently identify any structural irregularities that could account for this connectional pattern.

Lateral belt (ML/AL border) injections labeled cells in the core, medial belt, lateral belt, and parabelt (Figure 7). Injections labeled cells in the rostral and caudal sections of the medial belt with strong labeling of areas adjacent to the injection site in the lateral belt (Figure 12). Cells were also labeled strongly in the core, with the strongest connections in the core areas adjacent

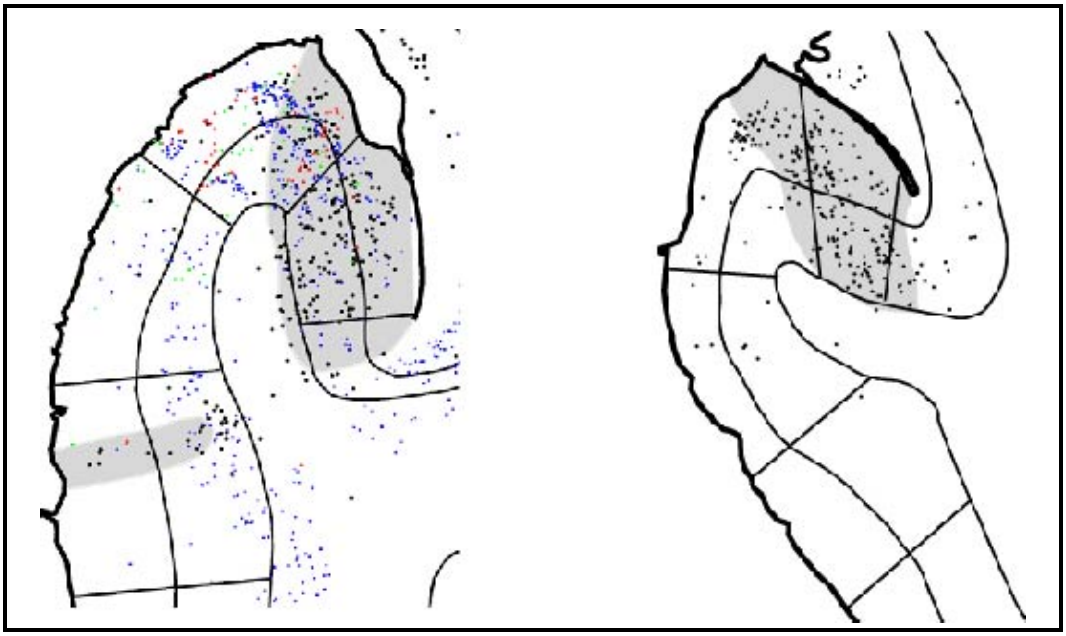

Figure 11. Case 01-37 left, 01-118 right, labeling of medial portion of the core both anterograde and retrograde.

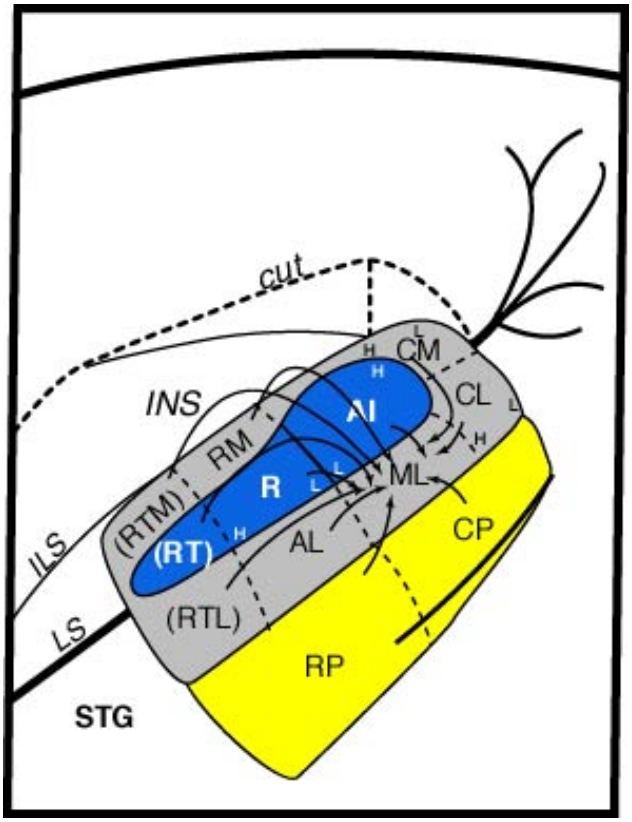

Figure 12. Summary figure of lateral belt (ML/AL border) injection connection pattern.

to the injection site and labeled cells in both the rostral and caudal regions of the parabelt (Figure 12).

Core (R) injections labeled cells in the core, medial belt and lateral belt (Figure 7). Injections into the caudal area of the R division of the core labeled cells strongly in R and A1, with less dense connections to the more rostral RT division of the core (Figure13). Rostral divisions of the medial belt and lateral belt were strongly labeled but interestingly there was no label found in the most caudal areas of the medial and lateral belts (CM and CL) (Figure13). There were only sparse connections to the rostral and caudal parabelt areas consistent with the current model (Figure 13).

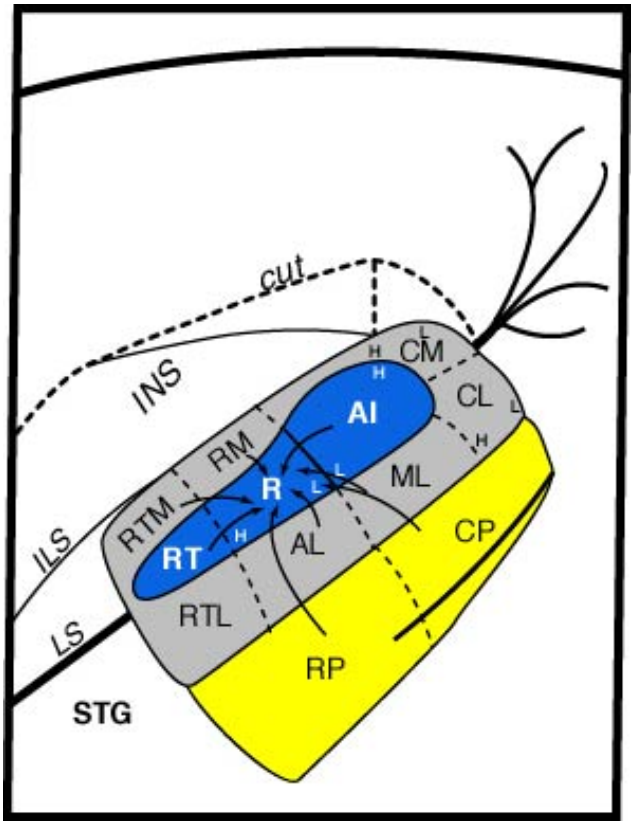

Figure 13. Summary figure of core (R) injection connection pattern.

Connections with the thalamus labeled primarily the dorsal division of the medial geniculate nucleus as well as the magnocellular division and suprageniculate, consistent with the connection patterns of belt areas (Figure 14).

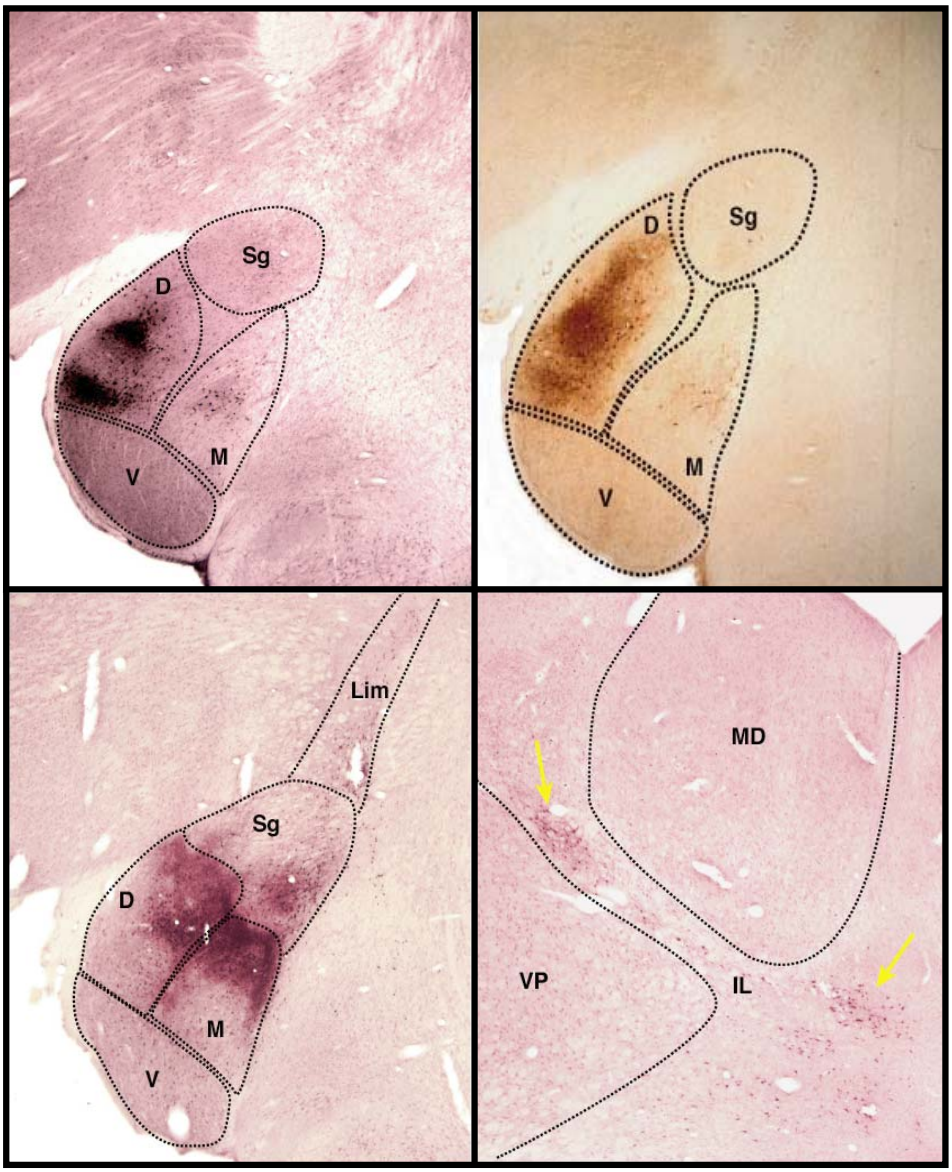

Figure 14. Thalamic labeling. Top left 01-118 CTB RM, top right 01-118 BDA RM more caudal, bottom left 01-89 CTB CM, bottom right 01-89 CTB label found in the intralaminar nuclei.

Reconstruction of CM injected sections is not yet complete, however based on preliminary findings there does appear to be support for differences in the connectional patterns of rostral an caudal medial belt areas. Case 01-118, which has a medial belt injection more caudal than 01-37 (RM), appears to have a similar connection pattern to that of case 01-37. Examination of the thalamus revealed similar distribution of label without the separation of dorsal and ventral patches in the dorsal medial geniculate and labeling found in the magnocellular and suprageniculate (Figure 14). Case 01-89 in which the injection is in area CM reveals a completely different labeling pattern in which there is heavy label in the dorsal part of the MGd and MGm extending into the suprageniculate, limitans and intralaminar nuclei, which have been shown to receive multisensory and somatosensory inputs.

An interesting banding pattern of anterograde label was found in the lateral belt from injections made in the rostral medial belt and this pattern was reflected in both CTB and BDA tracers (Figure 15). Injections into medial belt areas showed no connectional overlap with DY injections into somatosensory cortex regardless of whether the injections were made rostral or caudal (Figure 16).

CHAPTER IV

DISCUSSION

The working model of auditory cortex developed in recent years (Kaas & Hackett, 2000) divides the auditory cortex into three regions; core, auditory belt, and parabelt (Figure 1). The current study used both anatomical tracers and electrophysiological recordings to study the connections and organization of auditory cortex, specifically areas of the medial belt, which, due in part to the inaccessibility, have not been well studied. Findings from the rostral medial belt (RM) injection (01-37, 01-118) were consistent with the working model in that there were connections to all core areas (Kaas & Hackett, 2000), the strongest being to those areas adjacent to the injection site, as well as connections to both rostral and caudal areas of the parabelt (Hackett et al., 1998). In addition, area RM also had connections with all belt areas bordering the lateral side of the core (ML, AL, RTL). This finding represents a significant extension of the model. Connections of the more caudal ML area of the lateral belt were consistent with the model (Kaas & Hackett, 2000) and confirmed interconnections between the lateral belt and medial belt areas. Although all rostral and caudal areas of both the medial belt and the lateral belt showed connections with the ML injection, there were no connections to the caudal medial belt area from the more rostral RM injection. Injections into the rostral core area, R, revealed sparse parabelt connections, consistent with previous findings (Hackett et al., 1998), but did not project to either the caudal medial or caudal lateral belt areas.

Overall, the findings support the hypothesis that the rostral medial belt fields are functionally distinct from the lateral belt fields. The rostral medial belt field (RM) was found to project broadly to both rostral and caudal divisions of the lateral belt and parabelt. This is consistent with previous findings that RM is unique in expressing no rostral caudal topography with respect to the parabelt (Hackett et al., 1998). By comparison, the connections of the lateral belt fields tend to favor either rostral or caudal divisions of auditory cortex (Hackett et al., 1998). This rostrocaudal

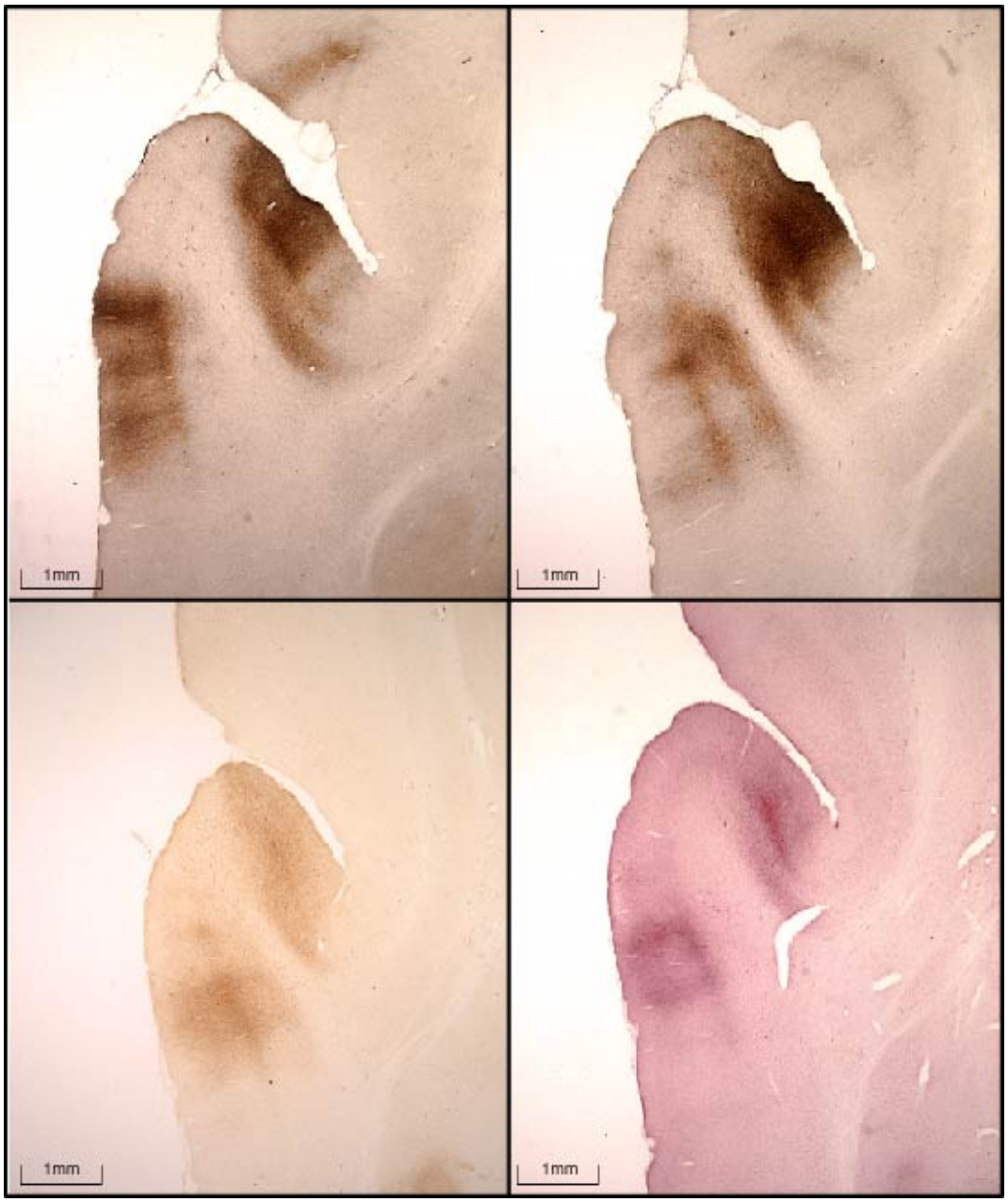

Figure 15. Anterograde banding of lateral belts. Top left 01-37 BDA, top right 01-37 BDA, bottom left 01-118 BDA, bottom right 01-118 CTB.

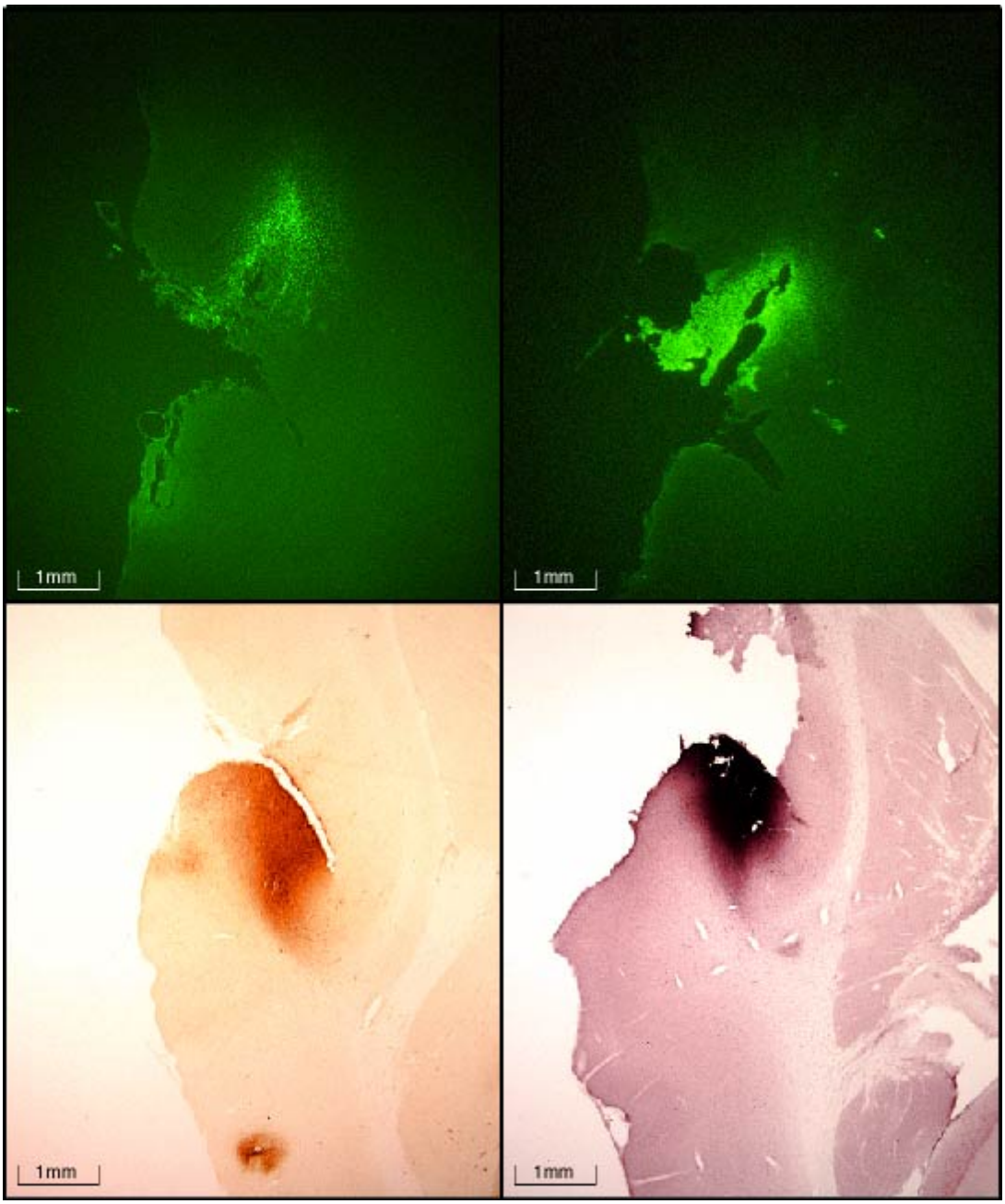

Figure 16. Case 01-118. Top left DY somatosensory injection, top right more caudal DY somatosensory label, bottom left rostral medial belt BDA injection, bottom right more caudal medial belt CTB injection.

topography is consistent with the proposal that the auditory system can be divided into two functionally distinct pathways, one arising from rostral areas the other from caudal areas (Kaas & Hackett, 1999). The rostral areas are considered to contribute to a non-spatial pathway similar to the ventral what' stream of the visual system, and the caudal areas a part of a spatial pathway similar to the dorsal 'where' stream of the visual system (Ungerleider & Mishkin 1982; Kaas & Hackett 1999). Distinct 'where' and 'what' pathways have gained much support in visual and somatosensory systems (Kaas & Hackett, 1999) and considering that similar tasks are required by the auditory system it would be natural to suspect that such functional specialization exists in the auditory system as well. Further evidence for functional specialization in the medial belt, and for the dual streams hypothesis, comes from recent studies that suggest auditory and somatosensory convergence in CM (Schroeder et al., 2001). To investigate possible sources of this somatosensory input into CM, injections of DY were made into somatosensory cortex (Figure 16). Due to the unique location of CM between somatosensory cortex and auditory core and belt areas (RM is buffered by insula), somatosensory cortex is a logical area to look at as a source of input. Upon examination of both rostral and caudal injections into the medial belt, label was not found to overlap with label from the somatosensory injection (Figure 16). It does not appear that somatosensory cortex is a source of input into CM. Injections made into CM do appear to support the hypothesis that multisensory and somatosensory nuclei in the thalamus are a source of somatosensory input in CM. CM injections revealed connections in the suprageniculate, limitans, medial pulvinar and magnocellular nuclei and intralaminar nuclei, all of which have been found to have in multisensory or at least somatosensory inputs (Figure 14). The suprageniculate has been found to be labeled after spinal cord injections, and the magnocellular nucleus is known to be multisensory as well as the pulvinar in general. Such connections have not been found for any lateral belt area.

Data from the current study of RM, and preliminary data based on the connections of CM, indicate that the medial belt fields are functionally distinct from the lateral belt fields, as well as revealing distinct connection patterns between rostral and caudal medial belt areas. The multisensory thalamic connections of CM appear to support the proposal that here are dual

spatial and non-spatial pathways in the auditory system. Future research will be designed to elaborate both of these issues based on architecture, connections, and neuron response properties.

REFERENCES

Atkin, LJ, Kudo M, Irvine DRF (1988) Connections of the primary auditory cortex in the common marmoset (Callithrix jacchus jacchus), J. Comp. Neurol. 268:235-248.

Gallyas F, (1979) Silver staining of myelin by means of physical development. Neurol. Res. 1:203-209.

Geneser-Jensen FA, Blackstad TW (1971) Distribution of acetylcholinesterase in the hippocampal region of the guinea-pig: I Entorhinal area, parasubiculum, and presubiculum. Z. Zellforsch. Mikrosk. Anat. 114:460-481.

Hackett TA, Stepniewska I, Kaas JH (1996) Thalamic connections of the parabelt auditory region in macaque monkeys. Soc. Neurosci. Abstr. 23:186.

Hackett TA, Stepniewska I, Kaas JH (1998) Subdivisions of the auditory cortex and ipsilateral cortical connection of the parabelt auditory cortex in macaque monkeys. J. Comp. Neurol., 394:475-495.

Hackett TA, Stepniewska I, Kaas JH (1998b) Thalamocortical connections of the parabelt auditory cortex in macaque monkeys, J. Comp. Neurol., 400,271-286.

Hackett TA, Preuss TM, Kaas JH (2001) Architectonic identification of the core region in auditory cortex of macaques, cimpanzees, and humans. J. Comp. Neurol. 441:197-222.

Jones EG, Burton H (1976) Areal differences in the laminar distribution of thalamic afferents in cortical fields of the insular, parietal, and temporal regions of primates. *Journal of Comparative Neurology*, 168:197-248.

Kaas JH, Hackett TA (1998) Subdivisions and levels of processing in primate auditory cortex. Audiol. Neuro-otol., 3:73-85.

Kaas JH, Hackett TA (1999) ‘What’ and ‘where’ processing in auditory cortex. Nat. Neurosci., 2(12):1045-1047.

Kaas JH, Hackett TA (2000) Subdivisions of the suditory cortex and processing streams in primates. PNAS 97(22):11793-11799.

Merzenich MM, Brugge JF (1973) Representaion of the cochlear partition on the superior temporal plane of the macaque monkey. Brain Res. 50:275-296.

Morel A, Kaas JH (1992) Subdivisions and connections of the auditory cortex in owl monkeys. J. Comp. Neurol. 318:27-63.

Panndya DN, Sanides F (1973) Architectonic parcellation of the temporal operculum in rhesus monkey and its projection pattern. Z. Anat. Entwicklungsgesch. 139:127-160.

Rauschecker JP, Tian B, Hauser M (1995) Processing of complex sounds in the macaque nonprimary auditory cortex. Science 268:111-114.

Rauschecker JP, Tian B, Pons T, Mishkin, M (1997) Serial and parallel processing in rhesus monkey auditory cortex. J. Comp. Neurol. 382:89-103.

Sakai ST, Inase M, Tanjii J (1996) Comparison of pallidothlamic and cerebellothalamic pathways in the monkey (Macaca fuscata): A double anterograde labeling study. J. Comp. Neurol. 368:215-228.

Schroeder CE, Lindsley RW, Specht C, Marcovici A, Smiley JF, Javitt DC (2001) Somatosensory input to auditory association cortex in the macaque monkey. J. Neurophysiol., 85:1322-1327.

Ungerleider LG, Mishkin M (1982) Two cortical visual systems. In Ingle DJ, Goodale MA, Mansfield RJW (eds). Analysis of Visual Behavior. Cambridge: MIT Press, pp. 549-586.

Wang, X. (2000) On cortical coding of vocal communication sound sin primates. Proc. Nat. Acad. Sci., USA, 97 (22), 11843-11849.